

Foundation Activation Deformation and Environmental Restoration of Goaf under Cyclic Dynamic Load of High-speed Railway

Sahil Kavita*

Universiti Teknologi MARA, Malaysia

**corresponding author*

Keywords: Cyclic Dynamic Load, Mined-Out Area, Foundation Activation Deformation, Environmental Restoration Treatment, Soil Settlement

Abstract: With the rapid development of China's economic development, more and more transportation infrastructure construction, the construction of railways and highways in many places will inevitably pass through the goaf, and the foundation of the goaf cannot be avoided, or an avoidance plan is adopted. The problem of roof stability in the mined-out area has become increasingly prominent as an unfavorable geological problem in railway construction when the land is occupied and the cost is relatively high. This study explored the foundation activation deformation and environmental restoration treatment of the mined-out area under the action of high-speed railway cyclic dynamic loads. This study divides the load values into 10N, 20N, 30N, 40N, 50N, and 60N. When the load is 50N, the maximum rate of soil settlement on the top of the cap is 90%. When the load is 60N, the soil settlement between the piles under the cap is 85%. Because the parameter reduction is the range ratio reduction, the reduction ratio needs to be determined according to the actual deformation of the project. The surface subsidence in the study area is 0.7m, and the reduction ratio when the surface subsidence is 0.7m is determined by three-dimensional numerical simulation. Control the characteristics of the soil surface humidity before the start of the experiment, and avoid the selected goaf zone because the surface humidity is inconsistent, which ultimately leads to a large difference in the experimental results. The experimental results show that with the increase of the load, the soil settlement between the top of the cap and the pile below the cap is gradually increasing: although the settlement is slightly different everywhere, the difference is very small. It can be seen that the platform is a rigid platform, under the load, the overall force, overall settlement, as the embankment load increases, the settlement curve changes from steep to slow, and eventually tends to grow steadily.

1. Introduction

1.1. Background and Significance

In China's railway construction, most of the areas involved are unsaturated soil foundations, among which expansive soils are widely distributed in the southwest of China. In ordinary railway construction, the influence of expansion deformation on the track operation period is often negligible: but in high-speed, heavy-load railways, because of the strict deformation control standards (post-construction settlement is less than 15mm), the deformation that may occur during the operation period is bound to give Driving brings huge hidden dangers.

Analyzing the influence of dynamic load on the deformation and failure of the mined-out area provides a reliable basis for the stability evaluation of the mined-out area and engineering treatment design, which is of great significance to ensure the safe operation of the railway within the design life. This study discusses the load transfer law and deformation characteristics of expansive soils of high-speed railways, which can provide effective guidance for the design and construction of high-speed railway roadbeds in remote areas, provide an important reference for foundation reinforcement design, and investigate and strengthen expansive soil foundations in remote areas Provide optimized program suggestions [1].

1.2. Related Work

Luiz Álvaro Oliveira Júnior discusses the mechanical properties of beam-to-column connections in precast concrete structures designed for buildings requiring rigid connections. In the connection, steel fiber reinforced concrete (SFRC), connecting rods and shear keys are used to establish a connection that can resist positive and negative moments. Under the two models, the mechanical properties of the proposed connection were evaluated through dynamic and reverse cycle tests: the overall model and the model consisting of precast concrete elements, which used 1% SFRC and splicing reinforcement connections to establish the continuity of the reinforcement. The results of the cyclic test show that this prefabricated beam-to-column connection has semi-rigidity and high strength (88% of the strength provided by the overall model). The results of dynamic tests show that the average damping ratio of unbroken connections is about 1.0% and decreases to about 0.7% after rupture [2]. Madhavi LG has studied the response of unreinforced and geosynthesized dry sand under static and dynamic loading conditions. His research used a large three-axis device that can test samples with a maximum size of 300 mm in diameter and 600 mm in height. The large sample size used in his research can overcome the boundary effect in the triaxial test of reinforced sand. A series of triaxial compression tests were conducted on unreinforced and reinforced sand samples to study the effect of geotextile reinforcement on the mechanical properties of sand. A layer of woven geotextile is used to reinforce the sand. In different tests, the number of enhancement layers varies from one to six. It was observed that under static conditions, with the addition of the geotextile layer, the peak shear strength, axial strain and stiffness at failure increased. The enhanced benefit rate increases with the number of layers, but decreases with the increase of confining pressure, indicating that the reinforcement layer is more effective under low confining pressure. The cyclic triaxial test was conducted at a frequency of 1 Hz and a cyclic load of 4 kN. Compared with unreinforced sand, the reinforced specimens showed a significantly higher dynamic modulus [3]. Ni J has established the calculation and prediction broaching model of disk broaching effect, tool scraping effect and cyclic contact characteristics to solve the problem of large hole broaching load calculation error and poor dynamic load prediction accuracy. Integrate the Johnson-Cook model, divide the cutting contour of each tool in detail, and calculate the circular effect on the broaching load. In addition, considering the contact state of the tool and the workpiece, the calculation of

broaching further optimizes the load model by considering the different proportions of cutting and scraping in each tool during the broaching process. Considering the cyclic contact characteristics of the number of teeth between the tool and the workpiece, the dynamic broaching load phase is accurately calculated by dividing the broaching process into three: the initial contact phase h of the workpiece and the tool teeth, the complete contact phase of the workpiece and the tool [4]. Li N believes that the filling layer self-compacting concrete (FLSCC) is a key material for the new China Railway Track System (CRTS), which is usually affected by the periodic dynamic loads of high-speed trains and various environmental temperatures during service. He conducted a series of indoor simulation experiments to study the impact resistance of FLSCC using Phi 75 mm Hopkinson pressure bar (SHPB) under cyclic bending load and different temperature conditions. The dynamic increase factor is introduced to evaluate the effect of strain rate on various mechanical properties of FLSCC, and the corresponding mechanism is explained. The results show that the dynamic increase factors of the compressive strength (DIF_c) and peak strain (DIF_ε) of FLSCC increase linearly with the logarithm of the strain rate, while the specific energy absorption increases exponentially with the strain rate. The impact resistance of FLSCC is greatly affected by cyclic bending loads and low temperatures. Strain rate sensitivity of FLSCC compressive strength at negative temperatures (-20 degrees Celsius) is weaker [5].

1.3. Innovation and Main Content

Comprehensive application of similar material simulation experiments, theoretical analysis, numerical simulation and other methods focuses on the impact of water and surface train dynamic loads on the deformation and damage of shallow goafs:

(1) Observation of deformation and evolution process of overburden overburden in goaf after shallow coal seam mining by similar material simulation experiment and its relatively stable state in the end. The overburden overburden in goaf is basically divided into two zones: collapse zone and In order to eliminate the hidden danger of re-activation of rock blocks in the collapse zone, the fault zone proposes a method of semi-filled grouting to treat the mined-out area, and its strength is measured by slurry ratio experiment, combined with the structural characteristics of the cemented cement paste, a concrete pile is established The mechanical model of the column and the falling stone cement is analyzed, and its failure mode is analyzed, and the mechanical conditions of its failure and instability are derived.

(2) Through the experimental research on the mechanical properties of rock specimens, the results show that the compressive strength and shear strength of the rock decrease with the increase of water content, but the degree of impact on different types of rock is different, and the impact on the strength of hard rock It is smaller, but has a greater impact on the weak rock, and the relationship between the elastic modulus and compressive strength of the concrete used in the arch is combined with the experimental results.

2. Goaf

2.1. Hidden Dangers Caused by Goaf

Coal resources have been an important strategic resource and material basis for China's economic and social development since ancient times. In recent years, driven by the rapid development of the national economy, human demand for coal resources has further increased, resulting in the widespread existence of many coal resource-rich areas, small coal kilns that are collectively or privately excavated by private individuals, leaving many goafs. Coal seam goafs, especially old goafs or privately excavated small goafs, as a complex geological body, have the

characteristics of concealment, suddenness, and complexity. The existence of these underground goafs has brought great importance to the upper public facilities Great safety hazard [6].

With the rapid development of China's economy, railway construction has also developed rapidly. Many railway sites inevitably need to cross some coal mining affected areas, and the excavation methods of many old kilns and small coal kilns in the Midwest are not standardized, and the protective structure Imperfect and unclear mining range, which is a safety issue in itself. If these mining disturbance areas left by mining activities are affected by some ground traffic loads, the mining disturbance areas may move and deform one step further. It even caused the destruction of ground transportation facilities and caused casualties [7].

2.2. High-Speed Railway Cyclic Dynamic Load

Choosing reasonable parameters to define damage variables is of great significance for studying the damage evolution characteristics of rock under the combination of static load and cyclic impact. Based on the combined dynamic and static loading test device, the combined load test of static load and cyclic impact is carried out on the rock. The method of rock or concrete damage variables under static load can be used to define the parameters of rock damage variables from three perspectives: whether they can characterize the evolution of rock dynamic fatigue mechanical properties, the damage caused by the first impact, and the final reasonable damage. The results of the selection study show that the residual strain and wave impedance can define the damage variable of the rock under the combination of static load and cyclic impact; compared with the wave impedance, the damage variable calculated by the residual strain is greatly affected by subjective factors [8].

Generally, when the additional stress in the ground is 10% of the self-weight stress at the corresponding position, it can be considered that the additional response to the foundation at this depth has little effect, and the additional stress in the soil layer below this depth is very small, and the foundation The effect of settlement is negligible. However, for different foundation forms and different depths of ground disturbance under different loads, under the dynamic load of railway trains, and considering that the subgrade is a goaf, the rock body above the goaf has underpressure in the falling area Actual, a lot of cracks, etc. Therefore, for the safety of railway design, the additional stress in the subgrade is 5% of the self-weight stress as an additional stress at a certain depth, and the impact on the subgrade at this depth is negligible [9].

2.3. Foundation Activation Method in Goaf

Because the factors affecting the stability of the mined-out area are very complex, and the influence of each factor is not the same but they are related to each other, and the signs and boundaries of the factors that distinguish the stability of the mined-out area are ambiguous, so it is difficult to use classical mathematics. The model analyzes such complex problems as the stability evaluation of mined-out areas. For the comprehensive evaluation of the stability of the mined-out area, the main methods currently used are fuzzy comprehensive evaluation method, expert weight method and force distribution, subgrade and mined-out area settlement law method, gray correlation analysis method, etc. [10].

(1) Fuzzy comprehensive evaluation method. Based on the field survey data, the factors closely related to the collapse are selected, and the two-level fuzzy comprehensive evaluation method is used to predict the risk of ground collapse by zones. Considering all the qualitative and quantitative factors that affect the stability of the mined-out area, a comprehensive evaluation method based on the analytic hierarchy process and the gray correlation method is proposed to evaluate the underground mined-out area, and then the stability correlation degree ranking and stability are obtained Sex level. The comprehensive weighting method is used to determine the comprehensive

weight, and combined with the fuzzy matter-element theory, a fuzzy matter-element model of goaf stability is constructed to evaluate the stability of goaf [11].

(2) Expert rights law. Taking the surface of the mined-out area under the railway as the research object, the finite element model of the railway and the mined-out area was established by finite element software to study the settlement and deformation law of the mined-out area under different working conditions. Then through the analysis of the factors affecting the stability of the mined-out area, a method for evaluating the stability of the mined-out area is established, and on this basis, the railway dynamic load is applied to evaluate the stability of the mined-out area. To study the safety and stability performance during railway operation [12-13].

(3) Law of force distribution, roadbed and goaf settlement law. Railway pile-slab composite embankment is the research object. Through the numerical simulation analysis of the subgrade stress mechanism, the relevant laws of the axial force of the pile body, the side friction resistance of the pile and the pile-soil stress are obtained. Conducted research on the goaf control project involved on the railway and controlled it during the construction process. After the construction was completed, the settlement, drilling and physical detection methods were used to evaluate and analyze the quality of the goaf under the high-speed railway. Through the experimental study on the ratio of different grouting materials, a reasonable grouting material and slurry ratio were determined. Taking the underlying goaf of the railway as an example, the distribution characteristics of the mined-out area of the mined-out area, the destruction process, mechanism and falling law of the surrounding rock of the mined-out area are analyzed, and the distribution characteristics of the mined-out area of the coal seam under the railway subgrade, Provides a basis for the effective management of goafs [14-15].

(4) Gray correlation analysis method. First of all, the danger degree of ground collapse is forecasted in different regions. Through the analysis of the stability time, safety depth, maximum sinking amount and maximum sinking speed of the mined-out area, the stability of the ground in the mined-out area is demonstrated. Based on the survey of goaf features and surface subsidence data, the mechanism of surface subsidence in goaf was analyzed, and the feasibility and safety of the line construction were evaluated. Based on the theory of subsidence characteristics of overlying rock strata in goaf area, using limited geological data, the stability of the goaf area of Baishudi tunnel is analyzed and evaluated, and the influence degree of goaf area on the tunnel is predicted. The elastoplastic finite element calculations of rock mass stability from two to three dimensions under specific projects are carried out. The formation displacement and deformation are analyzed and the subgrade deformation control index is obtained. Establish FLAC numerical simulation model to get the stress variation near the railway, and analyze the influence of iron ore underground mining on the stability of railway subgrade. According to the normative requirements, the safety distance between the line and the main goaf was quantitatively evaluated, and the shallow buried goaf balance arch theory was used to quantitatively evaluate the effect of the Xiaoyao goaf on railway stability [16].

2.4. Formula Used in Foundation Activation

(1) A model for predicting cumulative plastic strain should not only be able to consider the number of repeated loads. The main influencing factors also need to be considered. The expression of the model is as follows.

$$\varepsilon_p = a \left(\frac{\sigma_d}{\sigma_m} \right) N^b + \frac{N^b (m\sigma_d + a\sigma_m)}{\sigma_2 - \sigma_1} \quad (1)$$

Where: ε_p is the cumulative plastic strain, σ_d is the static deflection force of the soil, σ_m is the dynamic deflection stress caused by the traffic load, and N^b is the material parameter. Since the mined-out area may be located at different positions under the railway train, the depth of disturbance at different positions under the railway train is required. When a static load is added to the surface directly above the mined-out area, the relationship between the load and the stability of the mined-out area is derived, and the additional effect of the added load on the stability of the mined-out area is obtained [17].

(2) The dynamic deflection stress caused by train cyclic load is expressed as follows.

$$\sigma_d = \sigma_1 - \sigma_3 = \sqrt{\frac{1}{2}[(\sigma_{d1} - \sigma_{d2})^2 + (\sigma_{d2} - \sigma_{d3})^2 + (\sigma_{d4} - \sigma_{d3})^2]} \quad (2)$$

Calculate the dynamic deflection stress caused by the following vehicle load through the cyclic load through the finite element model, calculate the static deflection stress considering the physical and mechanical indexes of the soil layer, and then take the coefficient according to the test or experience. There is indeed a critical dynamic stress value for subgrade soil, which divides the cumulative deformation into two types: stable and destructive. The additional dynamic stress of the roadbed determines the magnitude of the cyclic stress ratio, which is also the cause of the additional deformation, and the greater the additional dynamic stress caused by the heavier the car, the greater the harm to the roadbed during driving. Therefore, the occurrence of overloading of heavy vehicles should be eliminated. Due to the relatively large cyclic stress that the shallow roadbed bears, fatigue softening effect is more likely to occur under this effect. Therefore, the quality of the shallow roadbed should be strengthened in the design and construction process to increase its strength and stiffness [18].

(3) The total cumulative plastic deformation in the soil subgrade. The surface of the bed and the body of the fine-grained subgrade are layered to finally calculate the cumulative plastic strain of each layer. The sum of the layers calculates the total cumulative plastic deformation of the soil subgrade.

$$D = \sum_{i=1}^n \varepsilon_p h_1 2 \left((\sqrt{3} V_1 h_1 + S) + \sum_{i=1}^n k T^3 \right) \quad (3)$$

A three-dimensional track subgrade specification model considering train load, rails, tracks and subgrade structures is established. Moving wheels are used to simulate trains to establish contact relationships between structural layers. Multi-source uniform viscoelastic artificial boundaries are established at the cross-section to deal with dynamic boundary problems. The boundary is based on a consistent viscoelastic artificial boundary. Using the ABAQL software as a platform, the user unit subroutine VUEI is implemented by changing the distance between the load point and the artificial boundary. The boundary is suitable for complex structures such as railway embankments. It has the characteristics of simplicity, good accuracy and stable parameters after reasonable correction according to the actual structure [19].

(4) According to the theory of effective consolidation stress, the shear strength of cohesive soil depends only on the effective stress in the consolidation state before the failure, and it develops faster from the consolidation state to the failure state. Its water content is too late to change, so the strength is too late to change., The expression formula is as follows.

$$q = c_m + \tan \alpha \quad (4)$$

$$q = c_1 \tan \alpha_1 + \frac{\alpha_1 + \alpha_3}{2} \sin(m\alpha_1 + n\alpha_2) \quad (5)$$

$$q = \frac{\alpha_1 - \alpha_3}{2} (f_1 - f_2) \quad (6)$$

The value in the fuzzy judgment set is the degree of membership corresponding to the stability level, and the value is used to determine the stability evaluation level. At present, there are mainly two types of maximum membership criteria and weighted calculation methods. In this paper, the criterion of maximum membership is used to judge. Therefore, according to the principle of maximum membership, the stability level of the mined-out area is considered as grade II, that is, the stability of the mined-out area is basically stable. (The judgment set X is used to evaluate and analyze the geological factors of the mining area, the hydrological factors, the parameters of the mined area itself, and the subsets of the other characteristic factors, and a fuzzy judgment matrix about the factor subsets of each factor can be obtained. Among the factors, rock mass structure and geological structure are non-quantitative expression factors, and rock quality indicators can be quantitatively expressed, which needs to be quantitatively calculated according to the formula [20].

(5) Finally, the calculation formula of the undrained shear strength determined by the consolidated undrained test index is as follows.

$$\sigma_f = c_m \frac{\cos \alpha}{1 - \sin \alpha} + \frac{1 + k_0}{2} \times \frac{\sin \delta}{1 - \sin \alpha} \quad (7)$$

As the excavation depth of the foundation pit increases, the lateral deformation of the retaining structure is inevitable, but how to develop the lateral deformation is the key to the stability of the foundation pit support system. -Generally speaking, the destruction of the envelope is a sign, so it is very important to monitor the excavation closely. Through monitoring, we can know the strength of the retaining structure, and can conduct back analysis on the design parameters, adjust the construction parameters in time, and guide the next excavation.

3. Goaf Experiment

3.1. Experimental Parameter Setting

The control of experimental parameters is shown in Table 1. In view of the effect of train vibration load on the mined-out area, due to the mining disturbance in the underground mined-out area, the structural characteristics of the formed "three-band" rock mass are inconsistent with the original mechanical parameters. Discount. Because the parameter reduction is the range ratio reduction, the reduction ratio needs to be determined according to the actual deformation of the project. The surface subsidence in the study area is 0.7m, and the reduction ratio when the surface subsidence is 0.7m is determined by three-dimensional numerical simulation.

Table 1. Control of the experimental parameters shown

| Control type | Fall zone | Crack zone | Bending band |
|-----------------|-----------|------------|---------------------|
| Elastic modulus | 1/2 | 1/10 | 1/3 |
| Cohesion | 1/2 | 1/10 | 1/3 |
| Poisson's ratio | 1/3 | 1/2 | Original parameters |

3.2. Experimental Design Conditions of Goaf

According to the design of the experiment, complete the implementation of the experiment as well as loading and data collection.

According to the test plan, the model devices and test components required for the test were made, including model pipe piles made of PPR tubes, settlement plates, observation standards, and the roof of the simulated goaf.

Carry out the implementation of model tests, including the filling of simulated limestone, the filling of simulated strong weathering and weak weathering sandstone, the embedding of monitoring components, and the pouring of the bearing plate.

After the model is produced and maintained, the model embankment is loaded with 6 levels of load, and various test data are collected and recorded at the same time.

3.3. Experimental Design Process

The load value is divided into 10N, 20N, 30N, 40N, 50N, 60N. The changes of the soil settlement between the top surface of the cap and the pile below the cap are studied separately. During the experiment, pay attention to the change of the soil layer humidity, measure the soil layer humidity value in the experiment, and the content should be controlled at 0.1g per square. The number of pile groups on the top surface of the cap and the bottom of the cap is set to 6 groups.

4. Analysis of Experimental Results of Foundation Activation

4.1. Summary of Experimental Data

The change of the top surface of the bearing cap with load is shown in Table 2. When using numerical simulation method to study the stability of goaf under railway load, it is very important to choose the calculation range of model reasonably. The size of the model has a certain relationship with the magnitude of the vibration energy. The energy of the train vibration is much smaller than the energy of the earthquake, so the value range can be correspondingly smaller.

Table 2. Variation of the top surface of the cap with load

| Load (N) Descent rate (%) Number of groups | 10 | 20 | 30 | 40 | 50 | 60 |
|--|--------|----|----|----|----|----|
| | Group1 | 53 | 61 | 73 | 81 | 90 |
| Group2 | 43 | 52 | 65 | 76 | 85 | 62 |
| Group3 | 37 | 44 | 53 | 60 | 70 | 57 |
| Group4 | 26 | 39 | 47 | 55 | 66 | 52 |
| Group5 | 20 | 34 | 42 | 48 | 59 | 47 |
| Group6 | 17 | 25 | 39 | 46 | 54 | 42 |

The change of soil settlement between piles under the cap with load is shown in Table 3. The main factors affecting the stability of the mined-out area are: geological factors, hydrological factors, factors in the mined-out area and other characteristic factors. Under the effect of railway load, the goaf will have further activation effects. Therefore, we need to consider the characteristics of the railway and the goaf and the relationship between them.

Table 3. Variation of soil settlement between piles under the cap with load

| Load (N) Descent rate (%) Number of groups | 10 | 20 | 30 | 40 | 50 | 60 |
|--|--------|----|----|----|----|----|
| | Group1 | 45 | 50 | 58 | 68 | 77 |
| Group2 | 37 | 40 | 49 | 57 | 70 | 78 |
| Group3 | 29 | 32 | 36 | 46 | 60 | 64 |
| Group4 | 18 | 26 | 29 | 35 | 51 | 54 |
| Group5 | 12 | 18 | 24 | 28 | 42 | 48 |
| Group6 | 8 | 14 | 19 | 24 | 31 | 39 |

4.2. Experimental Data Analysis

The change of the top surface of the bearing cap with the load is shown in Figure 1. In the figure, the vertical plastic deformation varies with the load. When the load level is 10, the plastic deformation basically develops within 3 hours, and there is almost no time effect, and the plastic deformation is only below 0.1 mm; when the load level increases At 20, 30 or even 40, the plastic deformation obviously has a cumulative effect with time, and the deformation time effect has already appeared. The amount of plastic deformation has also increased significantly compared to the 10 load level, increasing to 0.2mm ~ 0.4mm; when the load When the level is further increased to 0.6 or 0.7, the slope of the plastic deformation of the fill increases significantly with time compared to the smaller load level, and even shows an accelerated growth trend. The maximum plastic deformation is already close to 1mm; The fill was destroyed in almost a few minutes.

The stepped change of the top surface of the bearing cap with load is shown in Figure 2. It can be seen from the figure that the accumulative plastic strain at the top surface of the filling model increases with load level and is different from the elastic strain. The elastic strain increases linearly with the load level, while the plastic strain increases nonlinearly with the load level in the form of an exponential function. When the load is 60N, the soil settlement between the piles under the cap is 85%. When the railway line is directly above the mined-out area, the additional deformation value of the railway dynamic load to the mined-out area is the largest, followed by the working conditions when the railway line is parallel to the width, and the smallest is the railway line is directly above the boundary of the mined-out area.

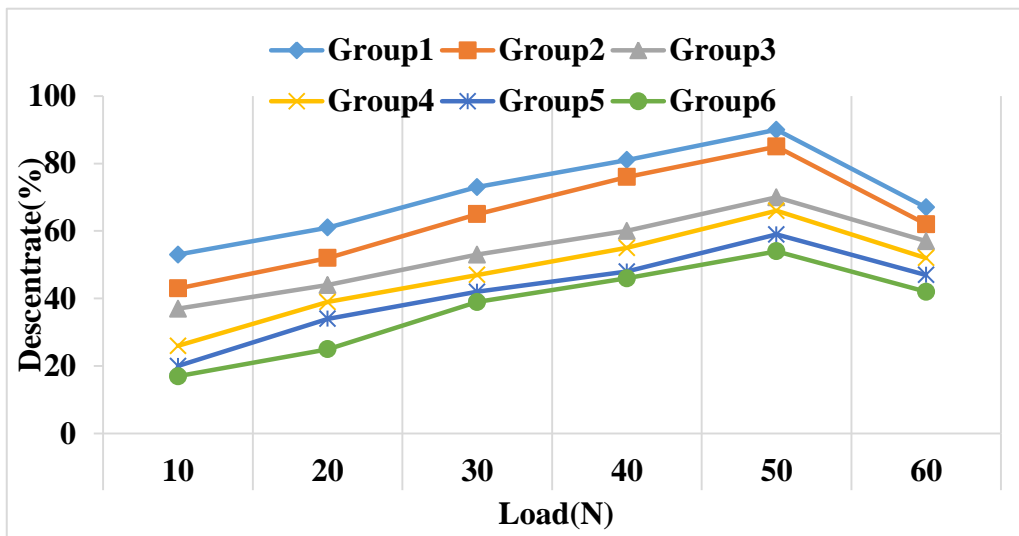


Figure 1. The change of the top surface of the cap with the load

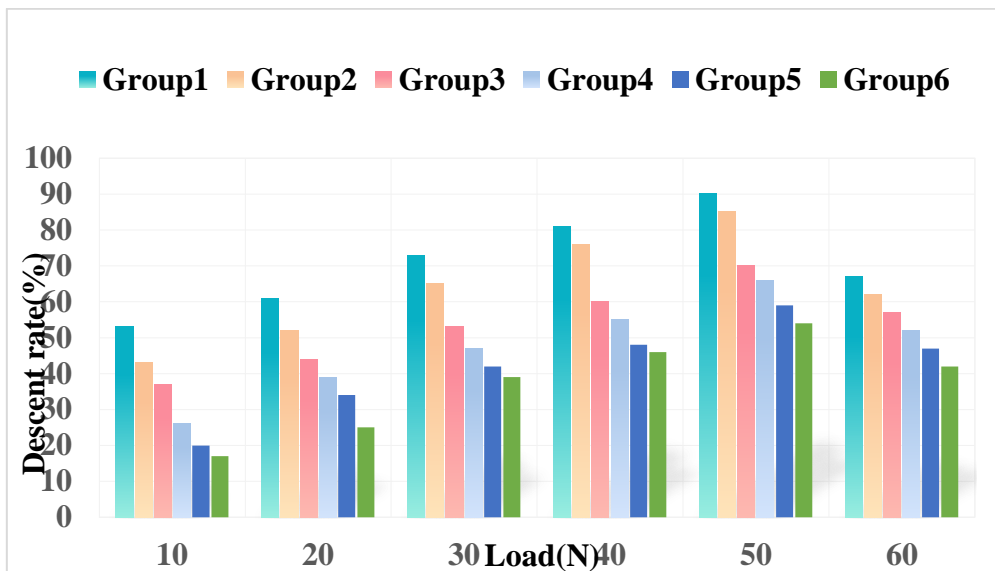


Figure 2. The stepped change of the top surface of the bearing cap with load

The change of soil settlement between piles under the cap with the load is shown in Figure 3. When the load is 60N, the soil settlement between the piles under the cap is 85%. Considering that the mined-out area is buried deep, and at the same time the project has obtained the distribution location of the remaining hidden loyalty area, the larger value of the treatment width calculated according to the above formula makes the treatment cost higher. When the existing railway hidden danger zone is treated, its treatment width can only be within the width of the road basic body and the surrounding belt, which can save cost while ensuring the stability of the roadbed and the safety of the train operation. Based on the existing construction experience, the determination of the treatment width was improved according to the specific conditions of the project. The main factors affecting the cumulative plastic strain of subgrade soil are: the static strength of the dynamic deviated stress soil, the type of soil and the number of repeated load cycles. For a given subgrade soil state and traffic conditions, except for the external dynamic deflection stress, other parameters are fixed, so the main method to control the cumulative plastic strain or deformation is to limit the dynamic deflection stress in the subgrade soil to an acceptable Level. The displacement response of

railway train dynamic load has obvious time-history characteristics and three-dimensional characteristics. The difference of train running position or time will make the vertical displacement of the surface above the goaf different.

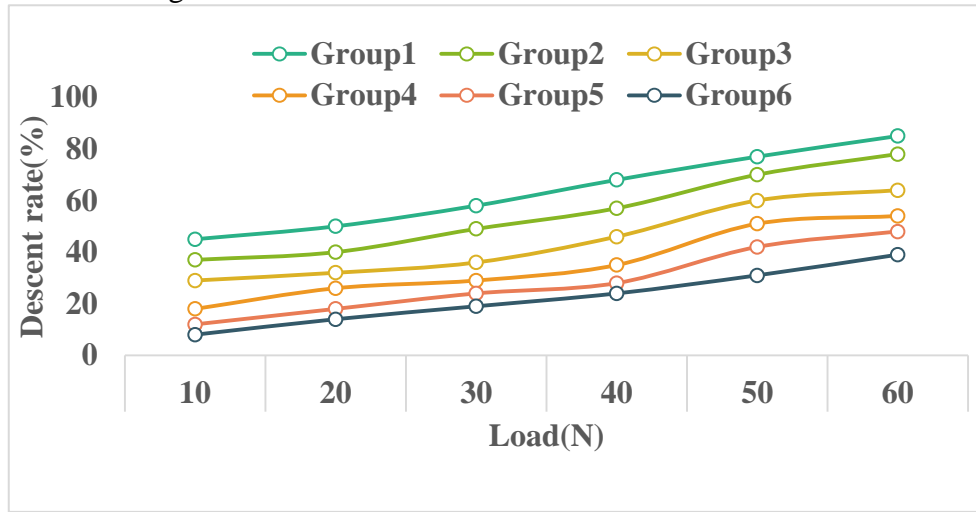


Figure 3. Variation of soil settlement between piles under the cap with load

The amount of change in soil settlement between piles under the cap with the trapezoid of the load is shown in Figure 4. In the process of load application, the first role is the lateral friction resistance of the upper rock layer. With the increase of the pile top load, the lateral friction resistance of the middle and lower rock layer is exerted. The same-the lateral friction resistance at the depth increases with the increase of the pile top load, and the degree of lateral friction resistance of different rock layers varies. The order of friction resistance is plain fill, strong weathered mudstone, and moderately weathered mudstone. Because plain fill is thicker and the side friction resistance is smaller, the main deformation in the early stage of the applied load occurs in the plain fill. With the downward transmission of the load, the side friction resistance of the strongly weathered mudstone plays a role. It can be drawn from the figure that the deformation of the middle weathered mudstone is very small. The resistance has not been exerted, and it mainly plays the role of bearing the pile end.

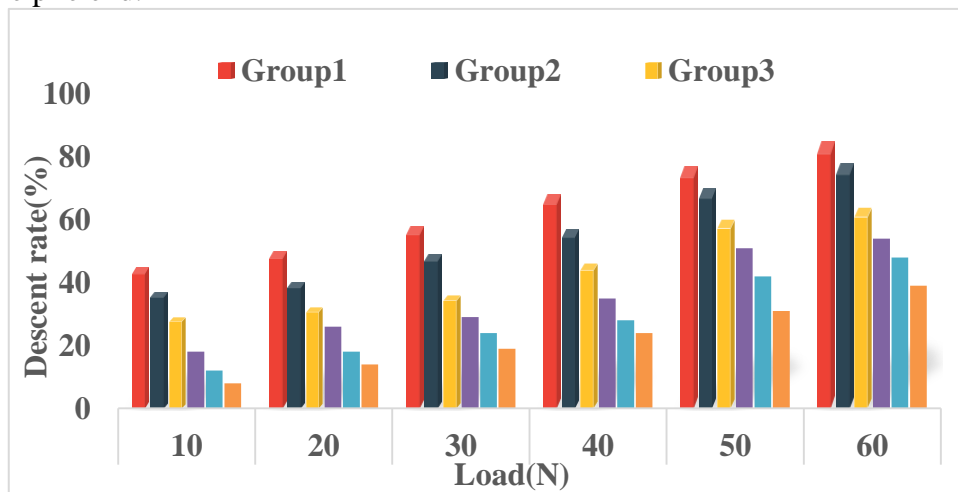


Figure 4. The amount of soil settlement between piles under the cap changes with the trapezoid of load

5. Conclusion

There are many problems faced by the high-speed railway passing through the mined-out area. There are relatively few research cases on the high-speed railway passing through the soft rock and coal mining subsidence area at the same time. Research methods. Therefore, systematic and in-depth research on this aspect has important theoretical significance and practical engineering value. This study relies on the high-speed railway section crossing the soft rock coal mining subsidence area, through surveys, theoretical calculations, numerical simulations, indoor tests and other methods, the stability of the goaf, detection of hidden areas, formation activation and deformation, treatment of hidden areas and reinforcement Systematic research has been carried out.

In this study, comprehensive exploration, theoretical calculation, numerical simulation and other methods were used to evaluate and analyze the stability of the goaf in Dapanjing, and at the same time, the distribution of the remaining hidden loyal zone was detected and the impact of the remaining hidden loyal zone on formation activation was analyzed. The treatment method of residual hidden trouble zone and the method of roadbed reinforcement are proposed, and the effect of roadbed reinforcement is verified.

This study analyzes in detail the distribution rules of dynamic and deviating stress of ballasted and ballastless track subgrades. On this basis, it predicts the cumulative deformation of soil subgrades when the high-speed railway group passes through double-block and plate ballastless tracks. This method combines finite element calculation and empirical fitting calculation model, which is easy to apply and provides technical support for the effective control of post-construction settlement of ballastless track subgrade of high-speed railway.

Funding

This article is not supported by any foundation.

Data Availability

Data sharing is not applicable to this article as no new data were created or analysed in this study.

Conflict of Interest

The author states that this article has no conflict of interest.

References

- [1] Liu Z N. *Accumulated Dynamic Strain Analysis of Heavy Load Railway Subgrade under Cyclic Loading*. *Journal of Railway Engineering Society*, 2018, 35(3):7-11.
- [2] Luiz Álvaro Oliveira Júnior, Daniel Lima Araújo, Debs M K E, et al. *Precast Beam–Column Connection Subjected to Cyclic and Dynamic Loadings*. *Structural Engineering International*, 2017, 27(1):114-126.
- [3] Madhavi L G, Nandhi V A M. *Static and cyclic load response of reinforced sand through large triaxial tests*. *Japanese Geotechnical Society Special Publication*, 2016, 2(68):2342-2346.
- [4] Ni J, Gu Z H, Yang X. *Dynamic load computing model for inner hole broaching*. *Zhejiang Daxue Xuebao*, 2017, 51(3):445-452.

- [5] Li N, Long G, Fu Q, et al. *Effects of Freeze and Cyclic Load on Impact Resistance of Filling Layer Self-Compacting Concrete (FLSCC)*. *KSCE journal of civil engineering*, 2019, 23(7):2908-2918.
- [6] Luo D, Su G, Zhang G. *True-Triaxial Experimental Study on Mechanical Behaviours and Acoustic Emission Characteristics of Dynamically Induced Rock Failure*. *Rock Mechanics and Rock Engineering*, 2020, 53(3):1205-1223.
- [7] Du K, Tao M, Li X B, et al. *Experimental Study of Slabbing and Rockburst Induced by True-Triaxial Unloading and Local Dynamic Disturbance*. *Rock Mechanics & Rock Engineering*, 2016, 49(9):3437-3453.
- [8] Shan S J, Chuan L Z, Ying L G, et al. *Rheological characteristic of argillaceous weak intercalation under intermittent dynamic shear loads*. *journal of china coal society*, 2017, 42(7):1724-1731.
- [9] Pavlic V, Matesic L, Kvasnicka P. *Numerical modelling of the NGI-DSS test and cyclic threshold shear strain for degradation in sand*. *Granular Matter*, 2017, 19(2):37.
- [10] Anisimov A V, Krokhin I A, Likhoded A I, et al. *Dynamic loading and stress life analysis of permanent space station modules*. *Mechanics of Solids*, 2016, 51(6):660-671.
- [11] Liu X, Liu Y, He C, et al. *Dynamic stability analysis of the bedding rock slope considering the vibration deterioration effect of the structural plane*. *Bulletin of engineering geology and the environment*, 2018, 77(1):87-103.
- [12] Huang Q, Huang H W, Ye B, et al. *Dynamic response and long-term settlement of a metro tunnel in saturated clay due to moving train load*. *Soils & Foundations*, 2017, 57(6):1059-1075.
- [13] Karacali O. *A New Perspective on Cyclic Loading Behavior Analysis of ATSP-Adjustable Telescopic Steel Prop S235GT Material Used in Structural Engineering*. *Acta Physica Polonica*, 2016, 129(4):436-438.
- [14] El Messiry M, Mohamed A. *Analysis of cyclic load die forming for woven jute fabric 3D reinforcement polymeric composites*. *Journal of Industrial Textiles*, 2018, 47(7):1681-1701.
- [15] Kiptoo D, Aschrafi J, Kalumba D, et al. *Laboratory Investigation of a Geosynthetic Reinforced Pavement Under Static and Dynamic Loading*. *Journal of testing and evaluation*, 2017, 45(1):76-84.
- [16] Zhang Z D, Li G Y. *Experimental study on particle breakage behaviors of rockfill under cyclic loadings*. *Yantu Gongcheng Xuebao/chinese Journal of Geotechnical Engineering*, 2017, 39(8):1510-1516.
- [17] Jamadin A, Ibrahim Z, Jumaat M Z, et al. *Effect of High-cyclic Loads on Dynamic Response of Reinforced Concrete Slabs*. *Ksce Journal of Civil Engineering*, 2019, 23(3):1293-1301.
- [18] Matyunin V M, Orakhelashvili B M, Marchenkov A Y, et al. *Static, Dynamic, and Cyclic Strength of Stud Metal in Large Hydraulic Units*. *Inorganic materials*, 2016, 52(15):1520-1527.
- [19] Arias J L, Inti S, Tandon V. *Influence of Geocell Reinforcement on Bearing Capacity of Low-Volume Roads*. *Transportation in Developing Economies*, 2020, 6(1):1-10.
- [20] Pandya S, Sachan A. *Experimental Studies on Effect of Load Repetition on Dynamic Characteristics of Saturated Ahmedabad Cohesive Soil*. *International Journal of Civil Engineering Transaction A Civil Engineering*, 2019, 17(6):781-792.